Separation and Purification Technology 325 (2023) 124660

Contents lists available at ScienceDirect

Separation and Purification Technology

journal homepage: www.elsevier.com/locate/seppur

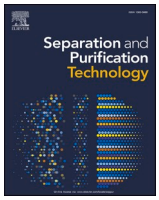

High D_2/H_2 selectivity performance in MOF-303 under ambient pressure for potential industrial applications

Hyunlim Kim [a], Seohyeon Jee [b], Jaewoo Park [a], Minji Jung [a], Raeesh Muhammad [a,*], Kyungmin Choi [b,*], Hyunchul Oh [a,c,*]

[a] Department of Chemistry, Ulsan National Institute of Science and Technology, Ulsan 44919, Republic of Korea
[b] Department of Chemical and Biological Engineering, Sookmyung Women's University, 100 Cheongpa-ro 47 gil, Yongsan-gu, Seoul, 04310, Republic of Korea
[c] Graduate school of Carbon Neutrality, Ulsan National Institute of Science and Technology, Ulsan 44919, Republic of Korea

ARTICLE INFO

Keywords:
Isotopologue separation
Kinetic quantum sieving
Metal-Organic Frameworks
1-D pores
Ultra-narrow pores

ABSTRACT

The commercial demand for D_2 is poised to increase significantly; however, the low natural abundance and the energy- and capital-intensive industrial separation (i.e., 24 K cryogenic distillation) will hamper future scientific and industrial growth in isotopologue separation. Alternatively, kinetic quantum sieving (KQS)-based adsorptive D_2 separation has been proposed recently, but the separation performance is reported mostly at near zero pressure or in the sub-few ten mbar range. Herein, an Al-based Metal-Organic Framework, MOF-303, with 1-D narrow-micro pores is studied for D_2/H_2 adsorptive separation at ambient pressure. Cryogenic thermal desorption spectroscopic analysis of MOF-303 confirmed that the synergetic effect of binding affinity & enhanced KQS (owing to molecular rearrangement of D_2 adsorbed phase at high pressure induced by strong D_2 confinement), along with D_2 partial condensation, leads to a significant increase in the D_2 uptake with increasing exposure pressure up to 1,000 mbar. Consequently, a remarkable selectivity of 21.6 at 25 K has been achieved even at an operating pressure of 1000 mbar, which is an industry-friendly condition. The observed D_2/H_2 separation selectivity is about ten times higher than that of the industrial cryogenic method (best selectivity of below 2.5 at 24 K), and comparable to the performance of the adsorbent materials already reported with low operating pressure, making adsorptive D_2/H_2 separation through MOF-303 an alternative for cryogenic industrial isotopologue separation.

1. Introduction

Separation of gases in pure or enriched form is important for many industrial processes, as different components of a mixture offer varying economic benefits [1–5]. Cryogenic distillation is commonly used for large-scale separation, but it accounts for about 10–15% of global energy consumption and contributes to atmospheric pollution [5–7]. As an alternative, adsorptive separation technology, which has a low energy penalty and is easy to operate, has emerged as a sustainable option [7–9]. Pressure swing adsorption (PSA) is widely used for the bulk separation of gases, but for adsorptive separation, the adsorption selectivity metric receives higher consideration [10]. However, uptake capacity and adsorption selectivity do not always go hand in hand, and the adsorbent selection process can become more complicated for isotopologue separation at high-pressure conditions.

D_2 is a scientifically and industrially relevant material, but its separation from H_2 is challenging due to its similar physical properties [11]. Developing an energy-efficient method for D_2 separation is crucial since the current industrial processes are both capital-intensive and consume a significant amount of energy. In this regard, research approaches based on adsorbents [12], membranes [13] and electrochemical pumping [14] have been explored for hydrogen isotope separation; however, owing to ease of operation the adsorptive separation garnered more attention. Separation of hydrogen isotopologue through the adsorptive separation is achieved by the nuclear quantum effects [15,16]. For that, porous adsorbents with ultra-narrow pores or stronger binding sites, such as activated carbon [17,18], covalent organic frameworks (COFs) [19], metal–organic frameworks (MOFs) [16,20], metal exchanged zeolites[11], and organic cages [21] and inorganic–organic hybrid cages[22], have been studied for H_2/D_2 separation. For example, Taufel et al., with the help of ultra-narrow pores MOF, MFU-4, achieved the D_2/H_2 Selectivity ($S_{D2/H2}$) of 7.5 at 10 mbar

* Corresponding authors.
E-mail addresses: raeesh@unist.ac.kr (R. Muhammad), kmchoi@sookmyung.ac.kr (K. Choi), hcoh@unist.ac.kr (H. Oh).

https://doi.org/10.1016/j.seppur.2023.124660
Received 13 May 2023; Received in revised form 15 July 2023; Accepted 23 July 2023
Available online 24 July 2023

exposure pressure (P_{ex}) [23]. He et al. studied the metal–organic cage, demonstrating the $S_{D2/H2}$ of 9.1 at the 200 mbar P_{ex} [22]. Ha et al. studied the Hoffman-type MOFs with unsaturated metal sites and achieved $S_{D2/H2}$ of 21.7 at 10 mbar P_{ex} [24]. Kim et al. functionalized MOF-74-Ni to tune the diffusion barrier and demonstrated the $S_{D2/H2}$ of 26 at 10 mbar P_{ex} [20]. These previous studies have shown high D_2/H_2 separation selectivity but at low exposure pressure, and there are only a few reports on high selectivity at higher pressure conditions, required for isotopologue separation through PSA. E.g., Li et al. studied Ni_2Cl_2BBTA having Ni^{2+} unsaturated site and demonstrated the $S_{D2/H2}$ of 4.5 at 1000 mbar P_{ex} [25]. Ren et al. studied SIFSIX-18-Cd similarly for the D_2/H_2 separation at 1000 mbar P_{ex} and obtained the $S_{D2/H2}$ of 5.1 [26]. Up to now, only Muhammad et al. achieved a significantly high $S_{D2/H2}$ of 25.8 at 1000 mbar P_{ex} using cobalt formate, but cobalt formate possesses a low surface area of 360 m^2/g [9,27]. To achieve high D_2 uptake and selectivity for industry-friendly purposes under high P_{ex}, an adsorbent with a high surface area and D_2 affinity is required. The adsorbents with a preferential binding affinity towards one component often show selective uptake, which becomes more profound at higher pressure, leading to increased selectivity. Therefore, we explore the isotopologue separation performance of MOF-303, an Al-based MOF [28], which exhibits exceptional stability, a stronger binding affinity towards D_2, and a greater D_2 uptake with increasing exposure pressure in comparison to H_2. This leads to a significant rise in $S_{D2/H2}$ at 1000 mbar. Thus, we carried out isotopologue separation studies using advanced cryogenic thermal desorption spectroscopy and 20 K low-pressure high-resolution volumetric gas adsorption instruments.

2. Experimental

2.1. Materials

Aluminum chloride hexahydrate ($AlCl_3{\cdot}6H_2O$) (ReagentPlus®, 99%), 3,5-pyrazoledicarboxylic acid (97%) were purchased from Sigma Aldrich. Methanol (99.8%) was purchased from DUKSAN. NaOH (Sodium hydroxide, 98%) was purchased from DAEJUNG.

2.2. Synthesis of MOF-303

Aluminum chloride hexahydrate (0.208 g, 0.862 mmol) and NaOH (0.026 g, 0.65 mmol) were dissolved in deionized water (7.5 mL). 3,5-pyrazoledicarboxylic acid (0.15 g, 0.862 mmol) and NaOH (0.026 g, 0.65 mmol) were dissolved in deionized water (7.5 mL). Then above two solutions were mixed with sonication for 10 min and heated at 100 °C for 15 h. After the completion of the reaction, the formed precipitate was separated and washed with deionized water and methanol three times with each and dried in a vacuum oven at room temperature.

2.3. Characterization

Thermogravimetric analysis (TGA) was carried out in N_2 atmosphere up to 800 °C with ramping rate of 5 °C/min. The porosity details were examined through N_2 sorption analysis estimated at 77 K using Autosorb iQ2. Specific surface area (SSA) was calculated using Brunauer–Emmett–Teller (BET) method, and pore volume using the adsorption branch of N_2 isotherm at relative pressure (P/P_0) of 0.95. Before the N_2 sorption isotherm measurement, the sample was outgassed at 80 °C for 12 h under dynamic vacuum. The Field Emission Scanning Electron Microscopy (FE-SEM, JSM-7600F JEOL) were carried out in GB_LOW mode, with a WD of 6.0 mm and scanned at 3 kV. Fourier transform infrared (FT-IR) spectroscopy was performed on a Thermo Fisher Scientific Nicolet iS50. Sample data were analyzed for ATR diamond mode measurements with 64 scans at a resolution of 4 cm^{-1}. The spectra were recorded in transmission mode.

2.4. Isotopologue separation

The isotopologue separation studies were conducted by measuring the H_2 and D_2 20 K low-pressure high-resolution isotherms and cryogenic thermal desorption spectra (TDS). Isotherms were measured using Autosorb iQ2-MP-XR equipped with cryo-cooler, from the temperature range of boiling temperature [D_2 (23 K) and H_2 (20 K)] to 60 K and up to 1000 mbar pressure, after activation at 80 °C for 12 h. TDS were measured using the home built advanced cryogenic thermal desorption spectrometer (ACTDS) equipped with high-resolution quadrupole mass spectrometer and cryo-cooler. ACTDS was calibrated using the TiH_2 and $Pd_{95}Ce_5$ metallic alloy. Single gas TDS measurement was done by exposing the sample with pure H_2 and D_2 gas at 1000 mbar and 298 K then cooling the sample to below boiling point of each gas. After achieving the equilibrium, all the gas molecules not adsorbed on the surface were pumped out. And then, the sample chamber was heated up to 293 K with ramping rate of 3 K/min. In the identical manner, TDS for isotopologue mixture was also measured using equimolar D_2 and H_2 mixture at specific exposure pressure and temperature. The uptake amount for D_2 and H_2 was calculated by integrating the area under the desorption curve. D_2 *vs.* H_2 selectivity ($S_{D2/H2}$) was calculated by using the following equation;

$$S_{D2/H2} = \frac{D_{2Ads}/H_{2Ads}}{D_{2gas}/H_{2gas}}$$

As, during the adsorption process, *the gas composition (partial pressure) does not vary due to the large chamber volume compared to the sorption amount*; hence $D_{2(gas)}/H_{2(gas)} \approx 1$ and the $S_{D2/H2}$ can be estimated by calculating the adsorbed molar ratio of D_{2Ads}/H_{2Ads}. Desorption energy was calculated from the TDS spectra measured at different heating rates (1, 2, and 3 K min^{-1}) following the method of Falconer and Madix [29].

3. Results and discussion

MOF-303 [$Al(OH)(C_5H_2O_4N_2)$] is a hydrothermally stable MOF, consisting of Al based inorganic secondary building units and pyrazole organic linker.[28,30] It has 6.0 Å wide rhombus-shaped one-dimensional channels running along a-axis, and the shortest channel distance between pyrazole organic linkers is 3.2 Å in c-axis, Fig. 1(a and b) [28]. The synthesis of MOF-303 was performed by reported method elsewhere, [31] and was confirmed by measuring the powder x-ray diffraction analysis, TGA and specific surface area measurement. Sharp diffraction peaks appearing at low angles and matching diffraction pattern with simulated diffraction pattern, indicated that crystallinity is well established (Fig. 1(c)).[30].

The obtained specific surface area of 951 m^2/g is consistent with the previously observed specific surface area of MOF-303 (989 m^2/g).[30] The microscopic analysis using FE-SEM has shown that the synthesized material primarily has cubic shape particle, Figure S1. The FT-IR spectra, shown in Figure S2, show the -N–H and -O–H stretching bands in the region of 3300–3400 cm^{-1} [32]. The bands observed at 1608 and 1388 cm^{-1} are observed due to –COO-Al coordination which leads to the framework formation.[32] The bands for -C = N and C–C stretching were observed at 1528 and 1480 cm^{-1}, respectively. The band for = N-N–H was observed at 1000 cm^{-1} [32]. The TGA profile of synthesized MOF-303 matches well with the previously reported literature[33] and shows two weight loss steps, first up to 130 °C due to loss of solvents and moisture, and second mass loss about 400 °C is caused by framework decomposition, Figure S3. The sharp rise in N_2 uptake at low relative pressure (P/P_0) and type-I N_2 isotherm shape indicates that material is microporous in nature, Fig. 1(d). The pore volume, using the adsorption branch of N_2 isotherm, was calculated to be 0.38 cc/g at P/P_0 of 0.95.

The H_2 and D_2 single component sorption isotherms were measured to access the uptake behavior under similar experimental condition. The

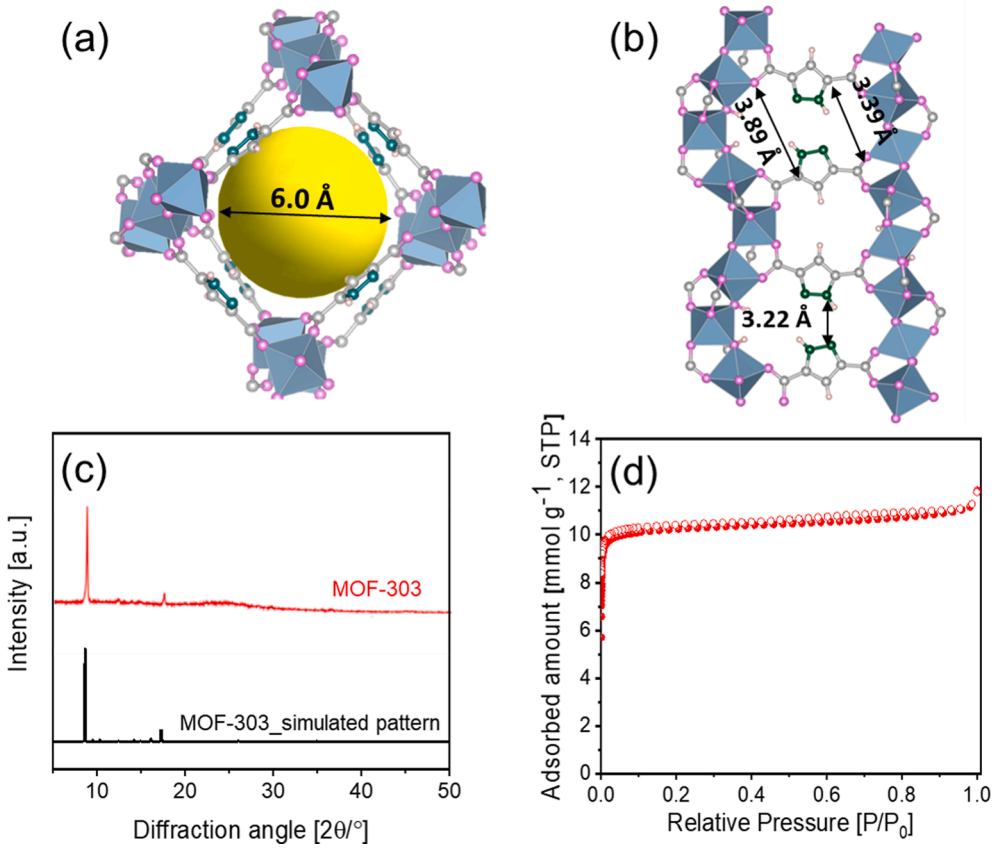

Fig. 1. Framework structure of MOF-303: (a) view of one-dimensional pore along 'a' axis and (b) two cavities of 3.39 and 3.89 Å present in the pore wall, and 3.22 Å is the shortest distance between the closest pyrazole units. (c) X-ray diffraction pattern, and (d) N_2 sorption isotherm of MOF-303.

isotherms measured at condensation point (boiling temperature and 1000 mbar), showed the maximum D_2 uptake of 20.1 mmol/g which was higher than 2.6 mmol/g of H_2 total uptake (17.5 mmol/g), Fig. 2 & Figure S4. With the rise in temperature to 40 K and 60 K the uptake of D_2 and H_2 both decreases, which is typical sorption behavior. However, the sorption hysteresis exhibits a unique trend, showing only at 40 K isotherm, Fig. 2. The hysteresis should also exist in H_2 (20 K) and D_2 (23 K) isotherms under low pressure (similar uptake region at 40 K) but it is simply not observable due to the resolution limitation. As shown in Fig. S4 (a), gas adsorption starts directly over 1 mbar because of the fast adsorption at a very low temperature of 20/23 K, and thus adsorption and desorption differences below 1 mbar (where hysteresis is expected) are impossible to validate. The observed weak sorption hysteresis is likely attributed to the presence of a small aperture (3.22 ~ 3.89 Å) on the side of the channel (Fig. 1(a & b)). This phenomenon may lead to an enhanced Kinetic Quantum Sieving (KQS) effect. At 60 K, on the other hand, the observed weak sorption hysteresis disappears, and the isotherm follows a conventional reversible trend, Fig. S4(c). The absence of hysteresis at this temperature suggests negligible Kinetic Quantum Sieving (KQS) effect.

In order to gain a better understanding of the role of binding sites in MOF-303 for isotopologue separation, we conducted TDS measurements. Fig. 3 displays the pure gas TDS (H_2 and D_2) data collected after exposure at 1000 mbar, with complete desorption of all adsorbed gases achieved by 70 K (and mostly by 60 K). The presence of distinct sorption/binding sites is evidenced by the observation of different

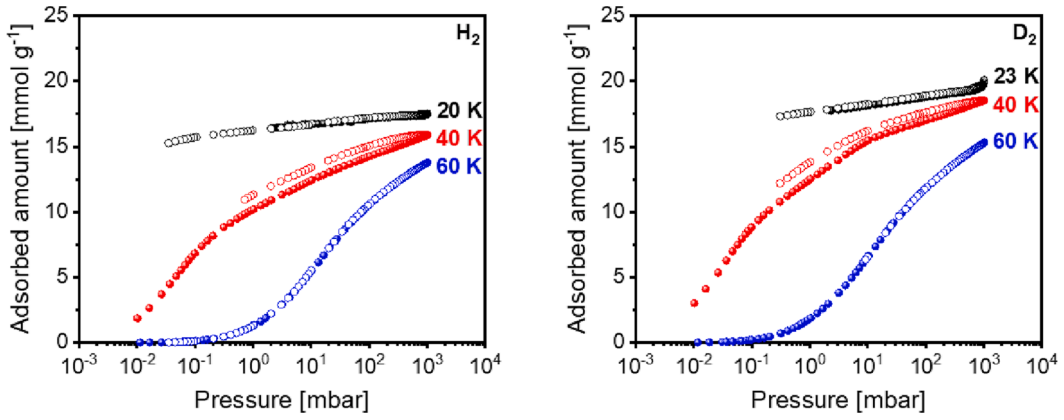

Fig. 2. D_2 and H_2 sorption isotherms for MOF-303; (a) H_2 sorption isotherms and (b) D_2 sorption isotherms, measured at various temperatures and up to 1000 mbar pressure (closed symbol; adsorption and open symbol; desorption).

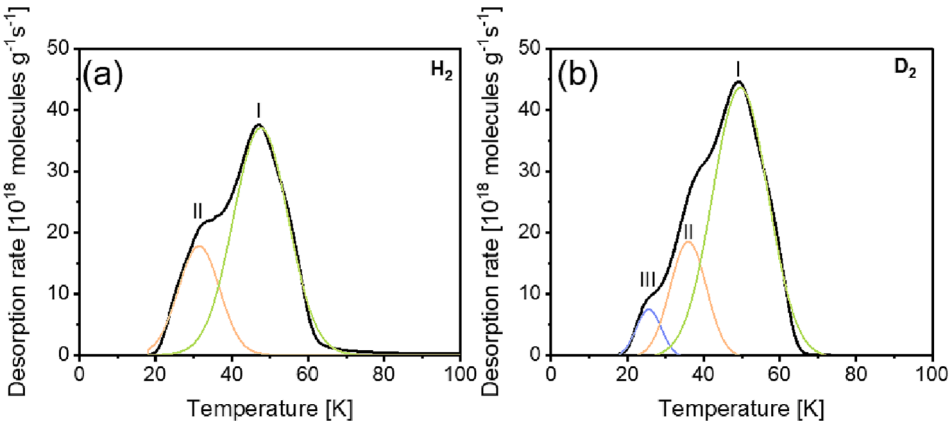

Fig. 3. Pure gas TDS measured after exposure of the sample with (a) H_2 and (b) D_2 at 1000 mbar.

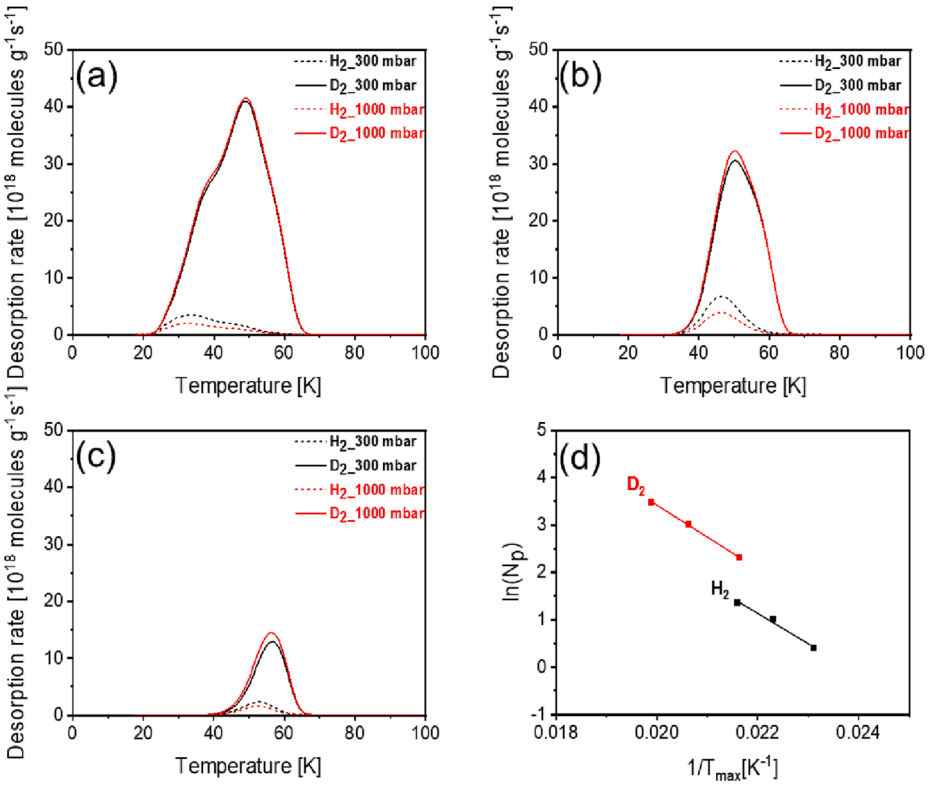

Fig. 4. TDS of D_2/H_2 equimolar mixture measured at varied exposure pressure (300 and 1000 mbar, and temperature (a) 25 K, (b) 40 K and (c) 50 K. 4(d) is the Falconer and Madix plots for the desorption of H_2 (black) and D_2 (red) from loaded MOF-303 at 40 K. (For interpretation of the references to colour in this figure legend, the reader is referred to the web version of this article.)

desorption peaks, with two peaks observed for H_2 and three peaks for D_2, indicating the existence of two identical sorption sites (sites I and II) for both gases, and an additional sorption site (site III) solely for D_2. The peak maxima for D_2 were found to be centered at 49 (site I), 39 (site II) and 25 K (site III) while for H_2 these were centered at 47 (site I) and 33 K (site II). The observation of shifted temperature peak maxima for desorption of D_2 indicates its stronger binding with MOF-303 in comparison to H_2. The observation of two binding sites can be associated with the adsorption of H_2 and D_2 in the cavities present in the pore walls, which is in line with the observation made by Chen *et al.*, where they have theoretically observed that the two cavities of MOF-303 acts as the two independent chelating sites for Th(IV) metal ions.[32] Third desorption peak (site III) only for D_2 may be ascribed to partial condensation of D_2 due to the stronger adsorbent-adsorbate interaction compare to H_2, which was also supported by the desorption maxima close to boiling temperature of D_2.

Real-time isotopologue separation performance and the impact of MOF-303's higher binding affinity for D_2 on $S_{D2/H2}$ were evaluated by exposing the sample to an equimolar D_2/H_2 mixture at various exposure pressures (300 – 1000 mbar) and temperatures (25, 40, and 50 K), as shown in Fig. 4 & Figure S5. Initially, the sample was exposed to an isotopic gas mixture pressure of 300 mbar at 25 K, which resulted in a significantly high intensity TDS signal for D_2, indicating that binding sites were predominantly occupied by D_2 due to its higher binding affinity. (Note that partial D_2 condensation may also influence this high desorption signal.) Consequently, there was a considerable increase in selective D_2 uptake compared to H_2. In Fig. 4(a) and Figure S5(a), it was observed that increasing the exposure pressure to 300 and 1000 mbar

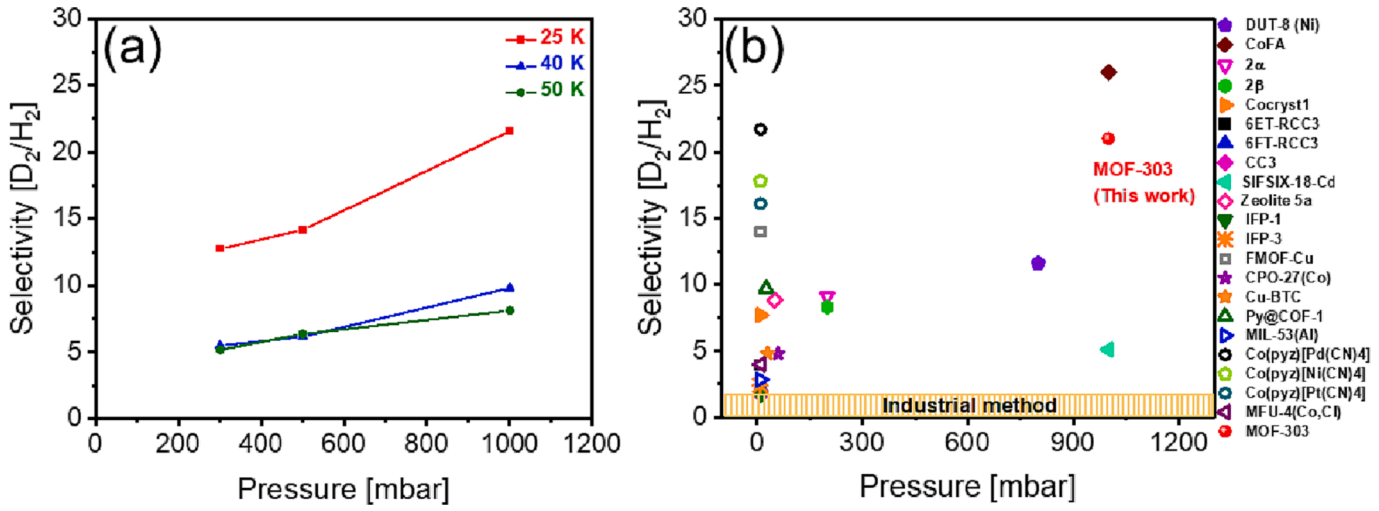

Fig. 5. (a) D_2/H_2 selectivity as function of pressure at 25, 40 and 50 K, (b) the comparison of D_2/H_2 selectivity of MOF-303 with the reported adsorbents.

resulted in a decrease in H_2 uptake while D_2 uptake increased. This increase in D_2 uptake was due to the strong confinement of D_2 molecules in the adsorbed phase, given its higher binding affinity with MOF-303. Molecular rearrangement resulting from the confined D_2 adsorbed phase favored the adsorption of the smaller-sized molecule (D_2) due to nuclear quantum effects. At 40 K, the reduction in H_2 signal was greater than that of D_2 and even more pronounced than at 25 K (as shown in Fig. 4(b) and S5(b)). The quantum sieving effects become the primary factor present, as the partial condensation effect disappears entirely at this temperature. With increasing pressure, the D_2 signal became stronger, whereas the H_2 signal weakened. These observations suggest that the small aperture on the side of the channel may influence the kinetic quantum sieving effect. At 50 K, the overall effect was reduced compared to that at 40 K, as depicted in Fig. 4(c) and S5(c).

To understand the desorption pattern of D_2 and H_2, the Falconer and Madix desorption plots were used based on the assumption that the remaining surface fractional coverages are the same at the desorption peak maxima irrespective of heating rate. The desorption energy was estimated using the below equation: [26]

$$\ln(N_P) = \ln(\nu.g(c_P)) - \left(\frac{E}{R}\right)\left(\frac{1}{T_P}\right)$$

Where N_p is the amplitude of desorption curve at peak maxima, ν is pre-exponential factor, $g(c_p)$ is arbitrary non-negative order expression for dependence of rate on surface coverage at peak maxima, T_P is the temperature at peak maxima, E is desorption energy and R is gas constant. The desorption curves were measured at the heating rates of 1, 2 and 3 K/min after the exposure of MOF-303 with equimolar mixture of isotopologue at 40 K, and shown in Figure S6. The desorption maxima shifted to the higher temperature with an increase in heating rate, indicating that the D_2 and H_2 desorption processes are thermally driven. The desorption energy was estimated from the slope (-E/R) of the plot of ln (N_p) versus $1/T_p$, Fig. 4(d). The desorption energy for H_2 and D_2 were determined to be 5.31 kJ/mol and 5.61 kJ/mol, respectively. The higher desorption energy for D_2 (heavier isotope) was attributed to kinetic quantum sieving and binding effects, which translate into its higher uptake capacity.

The real-time selectivity of the D_2 *vs.*H_2 mixture was estimated by calculating the ratio of D_2 and H_2 uptake amounts. As shown in Fig. 5(a), the selectivity increased with pressure at all temperatures. For instance, at 25 K and 300 mbar, the $S_{D2/H2}$ was estimated to be 12.7, and the maximum $S_{D2/H2}$ of 21.6 was achieved at 1000 mbar. This trend was consistent for 40 and 50 K, but the $S_{D2/H2}$ decreased with temperature. The high selectivity at 25 K could be attributed to the combined effects of binding affinity & enhanced KQS (owing to molecular rearrangement of D_2 adsorbed phase at high pressure indued by strong D_2 confinement) and partial D_2 condensation. Above 40 K, partial D_2 condensation effect is vanished, and thus leads to lower selectivity. The observed maximum $S_{D2/H2}$ of 21.6 at 1000 mbar of exposure pressure is significantly high compared to industrial H_2/D_2 separation technique ($S_{D2/H2}$ of below 2.5 at 24 K), and superior to many reported adsorbents like DUT-8(Ni)[16], Cocryst1[21], 6ET-RCC3[21], 6FT-RCC3[21], CC3[21], SIFSIX-18-Cd [26], Zeolite 5A[34], IFP-3[35], IFP-1[35], FMOF-Cu[36], Py@COF-1 [19], 2α[22], 2β[22], CPO-27(Co)[37], Cu-BTC[38], MIL-53(Al)[39], Co(pyz)[Pt(CN)4][24], Co(pyz)[Ni(CN)4][24], and MFU-4(Co,Cl)[40] (for selectivity comparison, please see Fig. 5(b)). The $S_{D2/H2}$ for Co(pyz) [Pd(CN)4][24] was comparable to that of MOF-303, while the $S_{D2/H2}$ of CoFA[9] was higher. However, the low exposure pressure in Co(pyz)[Pd (CN)4][24] and low surface area of CoFA[9] make these materials less attractive for industrial applications, giving MOF-303 an advantage over these. Moreover, the selectivity of MOF-303 remained unchanged even at high pressures of up to 1000 mbar, indicating its potential for efficient isotopologue separation under industrial conditions. Further, the comparison of selectivity and D_2 uptake of MOF-303 has been made with the reported adsorbents, as the uptake is directly linked with the product yield of the process. The D_2 uptake of MOF-303 was found to be superior among the compared adsorbents, Figure S7 and Table S1. These findings suggest that MOF-303 is a promising candidate for industrial applications, particularly at an exposure pressure of 1000 mbar.

4. Conclusion

This study investigated the potential of MOF-303, an aluminum-based metal–organic framework (MOF) with 1-D ultra-narrow pores, for hydrogen isotope separation. The results indicated that MOF-303 demonstrated a higher binding affinity and enhanced Kinetic Quantum Sieving (KQS) effect towards D_2, making it preferentially adsorbed over H_2. Furthermore, as the exposure pressure increased, the synergy effect, including partial D_2 condensation, became more significant, leading to a further enhancement of D_2 uptake. The observed isotopologue separation factor ($S_{D2/H2}$) of 21.6 at 1000 mbar was notably higher than the industrial technique of cryogenic distillation at below 2.5@24 K and among the best reported literature at high pressure. Due to its hydrothermal stability, excellent isotopologue separation ability, and suitability for industrial-scale operations at an exposure pressure of 1000 mbar, MOF-303 holds promising potential for adsorptive separation under industrial conditions.

CRediT authorship contribution statement

Hyunlim Kim: Writing – original draft. **Seohyeon Jee:** . **Jaewoo Park:** Investigation, Data curation. **Minji Jung:** . **Raeesh Muhammad:** Visualization, Project administration. **Kyungmin Choi:** Methodology, Writing – original draft. **Hyunchul Oh:** Conceptualization, Writing – review & editing, Supervision, Project administration, Funding acquisition.

Declaration of Competing Interest

The authors declare that they have no known competing financial interests or personal relationships that could have appeared to influence the work reported in this paper.

Data availability

No data was used for the research described in the article.

Acknowledgements

This work was supported by the National Research Foundation of Korea (NRF) grant program funded by the Korean Government (MSI) (Nos. 2022R1A2C3005978, RS-2022-00155422, 2022R1A2B5B010 0182612). R. M. acknowledges the Brain Pool Program funded by the Ministry of Science and ICT through the National Research Foundation of Korea (No. 2019H1D3A1A01071069).

Appendix A. Supplementary data

Supplementary data to this article can be found online at https://doi.org/10.1016/j.seppur.2023.124660.

References

[1] R.-B. Lin, L. Li, H.-L. Zhou, H. Wu, C. He, S. Li, R. Krishna, J. Li, W. Zhou, B. Chen, Molecular sieving of ethylene from ethane using a rigid metal–organic framework, Nat. Mater. 17 (12) (2018) 1128–1133.
[2] H. Wang, J. Li, Microporous metal-organic frameworks for adsorptive separation of C5–C6 alkane isomers, Acc. Chem. Res. 52 (7) (2019) 1968–1978.
[3] Y. Wu, B.M. Weckhuysen, Separation and purification of hydrocarbons with porous materials, Angew. Chem. Int. Ed. 60 (35) (2021) 18930–18949.
[4] R.S. Pillai, M.L. Pinto, J. Pires, M. Jorge, J.R.B. Gomes, Understanding gas adsorption selectivity in IRMOF-8 using molecular simulation, ACS Appl. Mater. Interfaces 7 (1) (2015) 624–637.
[5] D.-D. Zhou, J.-P. Zhang, On the role of flexibility for adsorptive separation, Acc. Chem. Res. 55 (20) (2022) 2966–2977.
[6] D.S. Sholl, R.P. Lively, Seven chemical separations to change the world, Nature 532 (2016) 435–437.
[7] P. Zhang, L. Yang, X. Liu, J. Wang, X. Suo, L. Chen, X. Cui, H. Xing, Ultramicroporous material based parallel and extended paraffin nano-trap for benchmark olefin purification, Nat. Commun. 13 (2022) 4928.
[8] J. Wang, Y. Zhang, P. Zhang, J. Hu, R.-B. Lin, Q. Deng, Z. Zeng, H. Xing, S. Deng, B. Chen, Optimizing pore space for flexible-robust metal-organic framework to boost trace acetylene removal, J. Am. Chem. Soc. 142 (2020) 9744–9751.
[9] R. Muhammad, S. Jee, M. Jung, J. Park, S.G. Kang, K.M. Choi, H. Oh, Exploiting the specific isotope-selective adsorption of metal-organic framework for hydrogen isotope separation, J. Am. Chem. Soc. 143 (2021) 8232–8236.
[10] R. Krishna, Adsorptive separation of CO2/CH4/CO gas mixtures at high pressures, Microporous Mesoporous Mater. 156 (2012) 217–223.
[11] R. Xiong, L. Zhang, P. Li, W. Luo, T. Tang, B. Ao, G. Sang, C. Chen, X. Yan, J. Chen, M. Hirscher, Highly effective hydrogen isotope separation through dihydrogen bond on Cu(I)-exchanged zeolites well above liquid nitrogen temperature, Chem. Eng. J. 391 (2020), 123485.
[12] J.Y. Kim, H. Oh, H.R. Moon, Hydrogen isotope separation in confined nanospaces: carbons, zeolites, metal–organic frameworks, and covalent organic frameworks, Adv. Mater. 31 (2019) 1805293.
[13] J. Coronas, Membrane application to gas separation of rare mixtures: A review, Journal of Membrane Science and Research 8 (2022).
[14] M. Lozada-Hidalgo, S. Zhang, S. Hu, A. Esfandiar, I. Grigorieva, A. Geim, Scalable and efficient separation of hydrogen isotopes using graphene-based electrochemical pumping, Nat. Commun. 8 (2017) 15215.
[15] M. Wahiduzzaman, C.F.J. Walther, T. Heine, Hydrogen adsorption in metal-organic frameworks: The role of nuclear quantum effects, J. Chem. Phys. 141 (2014), 064708.
[16] L. Bondorf, J.L. Fiorio, V. Bon, L. Zhang, M. Maliuta, S. Ehrling, I. Senkovska, J. D. Evans, J.-O. Joswig, S. Kaskel, T. Heine, M. Hirscher, Isotope-selective pore opening in a flexible metal-organic framework, Science, Advances 8 (2022) eabn7035.
[17] I. Krkljus, T. Steriotis, G. Charalambopoulou, A. Gotzias, M. Hirscher, H2/D2 adsorption and desorption studies on carbon molecular sieves with different pore structures, Carbon 57 (2013) 239–247.
[18] R. Muhammad, S. Kim, J. Park, M. Jung, M.E. Lee, J. Chung, H. Jang, H. Oh, Chemical affinity-assisted H2 isotope separation using Ca-rich onion-peel-derived nanoporous carbon composite, Materials Chemistry, Frontiers 5 (22) (2021) 8018–8024.
[19] H. Oh, S.B. Kalidindi, Y. Um, S. Bureekaew, R. Schmid, R.A. Fischer, M. Hirscher, A cryogenically flexible covalent organic framework for efficient hydrogen isotope separation by quantum sieving, Angew. Chem. Int. Ed. 52 (50) (2013) 13219–13222.
[20] J.Y. Kim, R. Balderas-Xicohténcatl, L. Zhang, S.G. Kang, M. Hirscher, H. Oh, H. R. Moon, Exploiting diffusion barrier and chemical affinity of metal–organic frameworks for efficient hydrogen isotope separation, J. Am. Chem. Soc. 139 (42) (2017) 15135–15141.
[21] M. Liu, L. Zhang, M.A. Little, V. Kapil, M. Ceriotti, S. Yang, L. Ding, D.L. Holden, R. Balderas-Xicohténcatl, D. He, R. Clowes, S.Y. Chong, G. Schütz, L. Chen, M. Hirscher, A.I. Cooper, Barely porous organic cages for hydrogen isotope separation, Science 366 (2019) 613–620.
[22] D. He, L. Zhang, T. Liu, R. Clowes, M.A. Little, M. Liu, M. Hirscher, A.I. Cooper, Hydrogen Isotope Separation Using a Metal-Organic Cage Built from Macrocycles, Angew. Chem. Int. Ed. 61 (2022) e202202450.
[23] J. Teufel, H. Oh, M. Hirscher, M. Wahiduzzaman, L. Zhechkov, A. Kuc, T. Heine, D. Denysenko, D. Volkmer, MFU-4 – A metal-organic framework for highly effective H2/D2 separation, Adv. Mater. 25 (2013) 635–639.
[24] J. Ha, M. Jung, J. Park, H. Oh, H.R. Moon, Thermodynamic separation of hydrogen isotopes using hofmann-type metal-organic frameworks with high-density open metal sites, ACS Appl. Mater. Interfaces 14 (2022) 30946–30951.
[25] X. Li, X. Wang, M. Li, J. Luo, Y. An, P. Li, J. Song, C. Chen, X. Feng, S. Wang, Highly selective adsorption of D2 from hydrogen isotopes mixture in a robust metal bistriazolate framework with open metal sites, Int. J. Hydrogen Energy 45 (2020) 21547–21554.
[26] J. Ren, W. Zeng, Y. Chen, X. Fu, Q. Yang, In silico screening and experimental study of anion-pillared metal-organic frameworks for hydrogen isotope separation, Sep. Purif. Technol. 295 (2022) 121286.
[27] Z. Wang, B. Zhang, M. Kurmoo, M.A. Green, H. Fujiwara, T. Otsuka, H. Kobayashi, Synthesis and characterization of a porous magnetic diamond framework, Co3 (HCOO)6, and Its N2 sorption characteristic, Inorg. Chem. 44 (2005) 1230–1237.
[28] N. Hanikel, X. Pei, S. Chheda, H. Lyu, W. Jeong, J. Sauer, L. Gagliardi, O.M. Yaghi, Evolution of water structures in metal-organic frameworks for improved atmospheric water harvesting, Science 374 (2021) 454–459.
[29] J.L. Falconer, R.J. Madix, Flash desorption activation energies: DCOOH decomposition and CO desorption from Ni (110), Surf. Sci. 48 (1975) 393–405.
[30] F. Fathieh, M.J. Kalmutzki, E.A. Kapustin, P.J. Waller, J. Yang, O.M. Yaghi, Practical water production from desert air, Sci. Adv. 4 (2018) eaat3198.
[31] N. Hanikel, M.S. Prévot, F. Fathieh, E.A. Kapustin, H. Lyu, H. Wang, N.J. Diercks, T.G. Glover, O.M. Yaghi, Rapid cycling and exceptional yield in a metal-organic framework water harvester, ACS Cent. Sci. 5 (10) (2019) 1699–1706.
[32] X. Chen, X. Liu, S. Xiao, W. Xue, X. Zhao, Q. Yang, A β-ray irradiation resistant MOF-based trap for efficient capture of Th (IV) ion, Sep. Purif. Technol. 297 (2022) 121517.
[33] Z. Zheng, H.L. Nguyen, N. Hanikel, K.-Y. Li, Z. Zhou, T. Ma, O.M. Yaghi, High-yield, green and scalable methods for producing MOF-303 for water harvesting from desert air, Nat. Protoc. 18 (1) (2023) 136–156.
[34] R. Xiong, R.B. Xicohténcatl, L. Zhang, P. Li, Y. Yao, G. Sang, C. Chen, T. Tang, D. Luo, M. Hirscher, Thermodynamics, kinetics and selectivity of H2 and D2 on zeolite 5A below 77K, Microporous Mesoporous Mater. 264 (2018) 22–27.
[35] S.S. Mondal, A. Kreuzer, K. Behrens, G. Schütz, H.-J. Holdt, M. Hirscher, Systematic experimental study on quantum sieving of hydrogen isotopes in metal-amide-imidazolate frameworks with narrow 1-D Channels, ChemPhysChem 20 (10) (2019) 1311–1315.
[36] L. Zhang, S. Jee, J. Park, M. Jung, D. Wallacher, A. Franz, W. Lee, M. Yoon, K. Choi, M. Hirscher, Exploiting dynamic opening of apertures in a partially fluorinated MOF for enhancing H2 desorption temperature and isotope separation, J. Am. Chem. Soc. 141 (2019) 19850–19858.
[37] H. Oh, I. Savchenko, A. Mavrandonakis, T. Heine, M. Hirscher, Highly effective hydrogen isotope separation in nanoporous metal–organic frameworks with open metal sites: direct measurement and theoretical analysis, ACS Nano 8 (2014) 761–770.
[38] F. Banijamali, A. Maghari, G. Schutz, M. Hirscher, Hydrogen and deuterium separation on metal organic frameworks based on Cu-and Zn-BTC: an experimental and theoretical study, Adsorption 27 (6) (2021) 925–935.
[39] J.Y. Kim, L. Zhang, R. Balderas-Xicohténcatl, J. Park, M. Hirscher, H.R. Moon, H. Oh, Selective hydrogen isotope separation via breathing transition in MIL-53 (Al), J. Am. Chem. Soc. 139 (2017) 17743–17746.
[40] J.S. Teufel, Experimental investigation of H2/D2 isotope separation by cryo-adsorption in metal-organic frameworks, DOI (2012).